



DIGITAL ACCESS TO SCHOLARSHIP AT HARVARD

Structure of dual receptor binding to botulinum neurotoxin B

The Harvard community has made this article openly available.
[Please share](#) how this access benefits you. Your story matters.

Citation	Berntsson, Ronnie P-A, Lisheng Peng, Min Dong, and Pål Stenmark. 2013. "Structure of dual receptor binding to botulinum neurotoxin B." <i>Nature communications</i> 4 (1): 2058. doi:10.1038/ncomms3058. http://dx.doi.org/10.1038/ncomms3058 .
Published Version	doi:10.1038/ncomms3058
Accessed	April 17, 2018 4:43:00 PM EDT
Citable Link	http://nrs.harvard.edu/urn-3:HUL.InstRepos:11879396
Terms of Use	This article was downloaded from Harvard University's DASH repository, and is made available under the terms and conditions applicable to Other Posted Material, as set forth at http://nrs.harvard.edu/urn-3:HUL.InstRepos:dash.current.terms-of-use#LAA

(Article begins on next page)

Published in final edited form as:

Nat Commun. 2013 ; 4: 2058. doi:10.1038/ncomms3058.

Structure of dual receptor binding to botulinum neurotoxin B

Ronnie P-A Berntsson¹, Lisheng Peng², Min Dong², and Pål Stenmark^{1,*}

¹Department of Biochemistry and Biophysics, Stockholm University, Stockholm, 10691, Sweden

²Department of Microbiology and Immunobiology, Harvard Medical School and Division of Neuroscience, New England Primate Research Center, Southborough, MA, 01772, USA

Abstract

Botulinum neurotoxins are highly toxic, and bind two receptors to achieve their high affinity and specificity for neurons. Here we present the first structure of a botulinum neurotoxin bound to both its receptors. We determine the 2.3 Å structure of a ternary complex of botulinum neurotoxin type B bound to both its protein receptor Synaptotagmin II and its ganglioside receptor GD1a. We show that there is no direct contact between the two receptors, and that the binding affinity towards Synaptotagmin II is not influenced by the presence of GD1a. The interactions of botulinum neurotoxin type B with the sialic acid 5 moiety of GD1a are important for the ganglioside selectivity. The structure demonstrates that the protein receptor and the ganglioside receptor occupy nearby but separate binding sites, thus providing two independent anchoring points.

Introduction

Botulinum neurotoxins (BoNT) are the most toxic substances known, with an LD₅₀ value of approximately 1 ng/kg¹. Seven distinct serotypes of BoNTs (A–G) exist^{2,3}. Due to their extreme toxicity, they are one of the top potential bioterrorism agents. However, members of botulinum neurotoxins (BoNT/A and B) are also extensively used therapeutically to treat numerous medical conditions, such as cervical dystonia, cerebral palsy, strabismus, hemifacial spasm and myofascial pain, as well as for cosmetic purposes^{4–6}.

These toxins are composed of three domains: the Light Chain (LC), the translocation domain (H_N) and the binding domain (H_C). The LC (~ 50 kDa), is a Zn-protease responsible for the cleavage of the SNARE (soluble NSF attachment protein receptor) proteins targeted by the toxin. SNARE proteins are central in synaptic vesicle exocytosis; cleavage of SNARE proteins by BoNTs inhibits acetylcholine release at the neuromuscular junctions⁷. H_N (~ 50 kDa) is responsible for transport of the LC over the endosomal membrane. H_C (~50 kDa) binds to receptors on nerve terminals^{2,8,9}. H_C is further divided into H_{CN} and H_{CC}, with H_{CN} being highly conserved and H_{CC} diverse in sequence. The receptors bound by H_{CC} and the final protein being targeted by the LC varies between serotypes. In general, BoNTs achieve their high affinity and specificity for neurons by binding two receptors;

*Corresponding author: stenmark@dbb.su.se, +46 8 163729.

Author contributions

R.P.-A.B. and L.P. performed the experiments. R.P.-A.B., M.D. and P.S. planned the experiments, performed data analysis, and wrote the manuscript.

Conflict of interests

The authors declare that they have no conflict of interests.

Accession codes

Atomic coordinates and structure factors have been deposited in the Protein Data Bank under accession code 4KBB.

gangliosides and one of the two synaptic vesicle proteins, synaptotagmin (Syt) or synaptic vesicle protein 2 (SV2). BoNT/A, D and E use SV2 as their protein receptor^{10–13}, BoNT/F might also utilize SV2^{14,15}, although this has not been functionally confirmed^{13,16}. BoNT/B and BoNT/G, bind Syt, both the Syt-I and Syt-II isoforms, as their protein receptors^{18–24}. In addition, the protein receptors of a BoNT subtype, type DC, are Syt-I and Syt-II¹⁷. Gangliosides bind in a ganglioside binding site (GBS), conserved in all serotypes except C and D, consisting of a SXWY motif^{14,15,25–30}. BoNT/C and D have in the same site an analogous GBS^{31–33}. Independent of which receptor the BoNT bind, the end result is similar; cleavage of SNARE proteins by the LC leading to muscle paralysis⁸.

Structures showing BoNT binding to either its protein receptor or gangliosides alone have been reported, including BoNT/B in complex with its protein receptor, synaptotagmin II (Syt-II)^{19,22}, BoNT/A with ganglioside GT1b²⁸, and BoNT/F with ganglioside GD1a³⁴. Structures are also available for BoNT/B, C, and D bound to smaller sugars^{25,31,33,35}. However, how BoNTs bind to both protein receptors and gangliosides simultaneously remains to be established at the structural level. Furthermore, no structure of BoNT/B bound to a complex ganglioside has previously been determined.

Here, we solve the structure of the first ternary complex of a BoNT bound to both its protein receptor and ganglioside. We determine the 2.3 Å structure of BoNT/B bound to Syt-II and the ganglioside GD1a. We show that the binding of GD1a does not influence the toxins affinity for Syt-II. Our results show that the two receptor binding sites are independent of each other.

Results

Overall structure of the complex

In a similar approach as previously reported, BoNT/B-H_C was constructed and purified as a fusion construct together with Syt-II²². This recombinant protein was then pre-incubated with GD1a, a major brain ganglioside known to bind BoNT/B³⁶, devoid of the ceramide part. Subsequent co-crystallization experiments yielded crystals that diffracted to 2.3 Å (Table 1). The structure was solved using molecular replacement. Residues 862–1291 of BoNT/B-H_C were visible in the electron density, with the exception of two flexible loops between residues 1151–1159 and 1245–1252. Well-defined electron density became visible during refinement, accounting for both the fused Syt-II toxin binding region (residues 45–59), and the entire GD1a ganglioside sugar (Fig. 1a). The remainder of the fused Syt-II was disordered and not visible in the electron density. The asymmetric unit contained two BoNT/B molecules, which were virtually identical (r.m.s.d. of 0.4 Å).

The structure shows that Syt-II is bound in a hydrophobic crevice on the tip of BoNT/B (Fig. 1a). The overall structure obtained in the ternary complex is virtually identical to the previously reported BoNT/B•Syt-II complex structures^{19,22}, demonstrating that simultaneous ganglioside binding does not cause any significant structure changes in BoNT/B.

Ganglioside binding to BoNT/B

This is the first structure of BoNT/B in complex with a complex ganglioside. The ganglioside binding site (GBS) on BoNT/B has been previously mapped, mainly through mutagenesis studies, and contains a conserved SXWY motif²⁶. The ternary complex structure revealed that GD1a indeed binds to this established GBS (Fig. 1 and 2). Four subunits of GD1a (Sialic acid (Sia5), Galactose (Gal4), N-acetylglucosamine (GalNAc3) and Sia6) make contacts to the GBS of BoNT/B (Fig. 1b). Sia5 forms hydrogen bonds to N1273, N1105, G1277 and Y1263, Gal4 to I1240, H1241, S1260 and E1190. GalNAc3 and

Sia6 form one hydrogen bond each, to E1190 and W1262 respectively. W1262 is furthermore forming crucial aromatic stacking interactions with Gal4. The remaining two subunits of GD1a, Glc1 and Gal2, do not interact with the GBS, but are still visible in the electron density due to the crystal packing to the second monomer in the asymmetric unit (Fig. 3). These crystal contacts are not biologically relevant; BoNT/B has previously been shown to have a single GBS²⁶. Key residues in the GBS mapped by previous mutagenesis studies, are highlighted with a star in the figure (Fig. 1b)²⁶.

We next compared the structure of BoNT/B•GD1a with the previously reported structures of BoNT/A•GT1b²⁸ and BoNT/F•GD1a³⁴ (Fig. 2). We found that there are significant differences in the position of most sugar moieties (Fig. 2a–d). However, the position of Gal4 is fairly conserved in all three structures. Interestingly GD1a has shifted one unit when compared with the previously determined structure of BoNT/B with bound sialyllactose²⁵ (Fig. 2e,f). This shift could indicate plasticity in the binding site, with different sugars being able to occupy the binding sites in different binding registers. Alternatively, the use of a partial mimic of the ganglioside or soaking could have influenced the position²⁵.

BoNT/B ternary complex

Importantly, the structure of BoNT/B in the ternary complex, does not undergo any significant conformational changes as compared to *apo* BoNT/B and the BoNT/B•Syt-II complex^{19,22,25} with an H_{CC} r.m.s.d. of 0.4 and 0.3 Å, respectively. Binding of the receptors induces only minor adjustments of the positions of side chains in the binding sites. For instance, W1262 moves slightly in the direction of Gal4. Gal2 and Glc1 are located between the membrane and the toxin, and are likely flexible. However, even allowing these moieties to be flexible, sterical and distance restraints likely prevents the ganglioside to reach the protein receptor in BoNT/B for a direct interaction. The closest distance between GD1a and Syt-II is 15 Å. E1190 interacts with GD1a and E1191 interacts with Syt-II, this is the closest connection between the binding sites. This result further establishes that the high binding affinity mainly is the product of two independent anchoring points, with no direct interactions between the binding sites or the receptors (Fig. 1 and 4). Furthermore, the toxins binding to the receptors impose sterical restraints on the interaction with the membrane (Fig 4).

GD1a does not influence the affinity for Syt-II

To further confirm the lack of allosteric effects between the dual receptors, we measured the binding affinity of rat Syt-II peptide (residue 40–60) to BoNT/B-H_C, without and with a pre-incubation with GD1a oligosaccharide. Isothermal titration calorimetry (ITC) gave a K_D of 0.14 ± 0.05 μM and 0.18 ± 0.06 μM, respectively (Fig. 5). The presence of GD1a did thus not significantly affect the binding affinity between Syt-II and BoNT/B, further indicating that there is no allosteric contribution in the binding of Syt-II and GD1a.

Discussion

The dual receptor concept for BoNT family toxins was proposed 27 years ago³⁷. The ternary structure, of BoNT/B bound to both Syt-II and GD1a concurrently, presented here, now proves the dual receptor model at the structural level. The structure demonstrates that the binding sites are separate and there are only minor changes in the structure upon binding of the receptors. There is no allosteric contribution in the binding of Syt-II and GD1a to BoNT/B. Due to the high sequence similarity between the recognition domains of Syt-I and Syt-II, it is likely that these receptors bind the toxin in a very similar way.

This is the first structure reported of BoNT/B bound to a complex ganglioside. Previous experiments have shown that GT1b and GD1a support BoNT/B binding, but that GD1b and GM1 bind substantially weaker^{21,36,38}. The structure presented here reveals the structural basis for this selectivity that arises from the interactions of Sia5. The Sia5 moiety is strongly bound to BoNT/B with key interactions for the overall binding of the ganglioside. Both GT1b and GD1a have a Sia5 moiety, whereas GD1b and GM1 do not, explaining the differences in affinity. Furthermore, K1265 and R1269, close to W1262, are well positioned to interact with the second sialic acid moiety present in GT1b (but not in GD1a), likely contributing to GT1b having even higher affinity than GD1a for binding BoNT/B^{25,36}.

The detailed description of dual receptor binding to BoNT/B can be used to develop toxin countermeasures targeting both sites simultaneously, thus benefitting from the high affinity achieved by binding multiple sites, as naturally occurring in the BoNTs.

Methods

Constructs and peptides

The cDNA encoding BoNT/B-H_C (residues 857 – 1291, GenBank: AB232927) was synthesized by GeneArt (Regensburg, Germany), with codon optimized for *E. coli* expression. The cDNA encoding mouse Syt II was generously provided by M. Fukuda (Ibaraki, Japan). The BoNT/B-H_C•Syt-II fusion construct was built by fusing BoNT/B-H_C directly to the N-terminus of Syt II (residues 8–61) by overlapping PCR, and subcloned into pET-28a vector at Nhe/XhoI site. The following additional residues from pET28 vectors were also expressed in the fusion protein:

N-terminus before BoNT/B-H_C: MGSSHHHHHSSGLVPRGSHMASM;

C-terminus after Syt II: VLEHHHHHH.

Peptide corresponding to the toxin-binding site in rat Syt-II (residue 40–60) was synthesized (>95% purity) by JPT Peptide Technologies GmbH (Germany).

Protein expression and purification

Double His-6 tagged BoNT/B-H_C – Syt-II was expressed in *Escherichia coli* (BL21 strain). The cells were grown in terrific broth medium containing 50 µg/mL kanamycin, and grown in 2 L flasks at 37°C, pH 7.0, with addition of air to mix the medium and maintain an excess of oxygen, to an OD₆₀₀ of ~1.5. The temperature was then lowered to 20°C, and expression induced by the addition of IPTG with a final concentration of 1mM. After over-night induction the cells were harvested and frozen in –80°C. For protein purification, the pelleted cells were thawed, resuspended to an OD₆₀₀ of ~100 in 50 mM KPi pH 7.5, 300 mM NaCl and 10% glycerol. Lysation was performed by passing the cell suspension 2 times through an Emulsiflex-C3 (Avestin, Germany) at 20 kPsi. Unlysed cells and cell debris was spun down via ultra-centrifugation at 4°C, 267k ×g for 60 min. The supernatant was collected, imidazole, pH 7.8, was added to a final concentration of 12 mM, and incubated with 0.5 mL Ni-NTA per 10 mL supernatant at 4°C for 60 min, rotating. The material was then packed in a disposable 10 mL column (BioRad), washed 20 column volumes with wash buffer (50 mM Hepes, pH 7.8, 300 mM NaCl and 45 mM imidazole, pH 7.8). The protein was then eluted using wash buffer supplemented with 500 mM imidazole, pH 7.8. Purification was then finished by running the protein over a Superdex 200 10/300GL size exclusion column, pre-equilibrated with 20 mM Hepes pH 7.0, 150 mM NaCl. The peak fractions were pooled and concentrated to 5.0 mg/mL, using a 30 kDa molecular weight cut off spin concentrator (Vivaspin). Glycerol was then added to a final concentration of 10%, and the protein was subsequently flash frozen in liquid nitrogen and stored at –80°C. Expression and

purification of BoNT/B-H_C for isothermal titration calorimetry (ITC) experiments was performed in the same way as BoNT/B-H_C – SytII, with the exception that BoNT/B-H_C was not frozen, and the final buffer in the size exclusion chromatography was 20 mM KPi pH 7.0, 150 mM NaCl.

Crystallization and structure determination

Purified protein was thawed, GD1a oligosaccharide (Elicityl, France) was added to a final concentration of 2.5 mM, and was subsequently crystallized using the vapor diffusion technique. Diffraction quality crystals grew from a solution containing 0.2 M MgCl₂, 0.1 M Hepes pH 7.0 – 7.2 and 20–24% PEG 6000. Crystals appeared between 8–12 weeks. For cryo protection, they were washed in mother liquor supplemented with 40% PEG 6000, and subsequently flash frozen in liquid nitrogen. Diffraction data was collected at 0.918 Å at beamline 14.1, BESSY, Berlin. The crystals diffracted to 2.3 Å, and were in space group P2₁. Data processing and reduction were carried out using XDS³⁹ and programs from the CCP4 suite⁴⁰. Relevant statistics are shown in Table 1. The structure was solved via molecular replacement, using the previously solved structure of BoNT/B as a search model (PDB code: 2NM1). A few cycles of refinement in Refmac5 and Phenix.refine^{41,42}, interspersed with model building using Coot⁴³, were needed to build the full model and its ligands. The final structure contains residues 862–1291, with the exception of two loops, 1152–1158 and 1246–1252 that had ambiguous electron density. At the N-terminus, 6 residues of BoNT/B are missing (MNSEIL), as well as the N-terminal tag. The Syt-II binding domain, residues 45–59, has well defined electron density, leaving residues 1–44 of Syt-II (which acts as a linker in this construct) flexible. Furthermore, the entire GD1a molecule is visible in the electron density. The highest resolution data, to 2.3 Å, had a twin fraction of ca 35 %, as analyzed via phenix.xtriage⁴². The structure was therefore refined using twin refinement. Another crystal form, in space group C2, diffracted to 2.6 Å and did not have twinning. The structure was also solved with this data, which was not twinned, and used for comparison with the higher resolution structure obtained from the twinned data. Final R_{work}/R_{free} of the untwinned data was 21.5 / 26.1 %. No substantial differences were observed between the two structures, and since the twinned data with higher resolution gave better final electron density, we choose to use that data for the final model building.

Isothermal titration calorimetry

Binding of synaptotagmin to BoNT/B-H_C was measured via isothermal titration calorimetry on a ITC200 (GE Healthcare) at 25°C and 1000 rpm. 200 µL of BoNT/B-H_C (typically concentrated to 10–25 µM, in 20 mM KPi pH 7.5, 150 mM NaCl) was added to the cell. In the case of GD1a oligosaccharide addition, 0.25 mM was added to the protein and incubated for 10 min on ice before adding the protein to the cell. Binding was measured upon addition of Syt-II peptide in a stepwise manner, typically 16 injections of 2.6 µL each, at a concentration of 10–15 times the protein concentration in the cell. The first titration was 0.5 µL, and was subsequently deleted in the data analysis. The analysis was performed using the software provided by the manufacturer.

Acknowledgments

This work was supported by grants from the Swedish Research Council (2010-5200), the Wenner-Gren Foundations and the Swedish Foundation for Strategic research to P.S, by an EMBO Long Term Fellowship and Marie Curie Actions (EMBOCOFUND2010, GA-2010-267146) to R.P.-A.B., and by the NIH grants 8P51OD011103-51 (to the New England Primate Research Center), 1R56AI097834-01 and 1R01NS080833-01 to M.D. We thank the Biomolecule Production Core at the NERCE (New England Regional Center for Excellence, NIAID U54 AI057159) for their assistance. We also acknowledge GE Healthcare for the use of the ITC200 machine in the demolab. We thank G. Widmalm and C. Hamark for discussions. We also thank the beamline scientists at BESSY, Berlin and at the Swiss Light Source, Switzerland for support.

References

1. Gill DM. Bacterial toxins: a table of lethal amounts. *Microbiol Rev.* 1982; 46:86–94. [PubMed: 6806598]
2. Schiavo G, Matteoli M, Montecucco C. Neurotoxins affecting neuroexocytosis. *Physiol. Rev.* 2000; 80:717–766. [PubMed: 10747206]
3. Smith TJ, et al. Sequence variation within botulinum neurotoxin serotypes impacts antibody binding and neutralization. *Infect Immun.* 2005; 73:5450–5457. [PubMed: 16113261]
4. Johnson EA. Clostridial toxins as therapeutic agents: benefits of nature's most toxic proteins. *Annu Rev Microbiol.* 1999; 53:551–575. [PubMed: 10547701]
5. Dolly JO, Lawrence GW, Meng J, Wang J, Ovsepian SV. Neuro-exocytosis: botulinum toxins as inhibitory probes and versatile therapeutics. *Curr Opin Pharmacol.* 2009; 9:326–335. [PubMed: 19394272]
6. Truong DD, Jost WH. Botulinum toxin: clinical use. *Parkinsonism Relat. Disord.* 2006; 12:331–355. [PubMed: 16870487]
7. Jahn R, Scheller RH. SNAREs--engines for membrane fusion. *Nat. Rev. Mol. Cell Biol.* 2006; 7:631–643. [PubMed: 16912714]
8. Montal M. Botulinum Neurotoxin: A Marvel of Protein Design. *Annu Rev Biochem.* 2010; 79:591–617. [PubMed: 20233039]
9. Swaminathan S. Molecular structures and functional relationships in clostridial neurotoxins. *FEBS J.* 2011; 278:4467–4485. [PubMed: 21592305]
10. Dong M, et al. SV2 is the protein receptor for botulinum neurotoxin A. *Science.* 2006; 312:592–596. [PubMed: 16543415]
11. Mahrhold S, Rummel A, Bigalke H, Davletov B, Binz T. The synaptic vesicle protein 2C mediates the uptake of botulinum neurotoxin A into phrenic nerves. *FEBS Lett.* 2006; 580:2011–2014. [PubMed: 16545378]
12. Dong M, et al. Glycosylated SV2A and SV2B mediate the entry of botulinum neurotoxin E into neurons. *Mol. Biol. Cell.* 2008; 19:5226–5237. [PubMed: 18815274]
13. Peng L, Tepp WH, Johnson EA, Dong M. Botulinum Neurotoxin D Uses Synaptic Vesicle Protein SV2 and Gangliosides as Receptors. *PLoS Pathog.* 2011; 7:e1002008. [PubMed: 21483489]
14. Fu Z, Chen C, Barbieri JT, Kim J-JP, Baldwin MR. Glycosylated SV2 and gangliosides as dual receptors for botulinum neurotoxin serotype F. *Biochemistry.* 2009; 48:5631–5641. [PubMed: 19476346]
15. Rummel A, et al. Botulinum neurotoxins C, E and F bind gangliosides via a conserved binding site prior to stimulation-dependent uptake with botulinum neurotoxin F utilising the three isoforms of SV2 as second receptor. *J Neurochem.* 2009; 110:1942–1954. [PubMed: 19650874]
16. Yeh FL, et al. SV2 Mediates Entry of Tetanus Neurotoxin into Central Neurons. *PLoS Pathog.* 2010; 6:e1001207. [PubMed: 21124874]
17. Peng L, et al. Botulinum neurotoxin D-C uses synaptotagmin I/II as receptors and human synaptotagmin II is not an effective receptor for type B, D-C, and G toxins. *J. Cell. Sci.* 2012; 125:3233–3242. [PubMed: 22454523]
18. Nishiki T, Ogasawara J, Kamata Y, Kozaki S. Solubilization and Characterization of the Acceptor for Clostridium-Botulinum Type-B Neurotoxin From Rat-Brain Synaptic-Membranes. *Biochim Biophys Acta.* 1993; 1158:333–338. [PubMed: 8251534]
19. Chai Q, et al. Structural basis of cell surface receptor recognition by botulinum neurotoxin B. *Nature.* 2006; 444:1096–1100. [PubMed: 17167418]
20. Nishiki T, et al. Identification of protein receptor for Clostridium botulinum type B neurotoxin in rat brain synaptosomes. *J Biol Chem.* 1994; 269:10498–10503. [PubMed: 8144634]
21. Nishiki T, et al. Binding of botulinum type B neurotoxin to Chinese hamster ovary cells transfected with rat synaptotagmin II cDNA. *Neurosci. Lett.* 1996; 208:105–108. [PubMed: 8859901]
22. Jin R, Rummel A, Binz T, Brunger AT. Botulinum neurotoxin B recognizes its protein receptor with high affinity and specificity. *Nature.* 2006; 444:1092–1095. [PubMed: 17167421]

23. Dong M, et al. Synaptotagmins I and II mediate entry of botulinum neurotoxin B into cells. *J Cell Biol.* 2003; 162:1293–1303. [PubMed: 14504267]
24. Rummel A, Karnath T, Henke T, Bigalke H, Binz T. Synaptotagmins I and II act as nerve cell receptors for botulinum neurotoxin G. *J Biol Chem.* 2004; 279:30865–30870. [PubMed: 15123599]
25. Swaminathan S, Eswaremoorthy S. Structural analysis of the catalytic and binding sites of *Clostridium botulinum* neurotoxin B. *Nat Struct Biol.* 2000; 7:693–699. [PubMed: 10932256]
26. Rummel A, Mahrhold S, Bigalke H, Binz T. The HCC-domain of botulinum neurotoxins A and B exhibits a singular ganglioside binding site displaying serotype specific carbohydrate interaction. *Mol Microbiol.* 2004; 51:631–643. [PubMed: 14731268]
27. Fotinou C, et al. The crystal structure of tetanus toxin Hc fragment complexed with a synthetic GT1b analogue suggests cross-linking between ganglioside receptors and the toxin. *J Biol Chem.* 2001; 276:32274–32281. [PubMed: 11418600]
28. Stenmark P, Dupuy J, Imamura A, Kiso M, Stevens RC. Crystal structure of botulinum neurotoxin type A in complex with the cell surface co-receptor GT1b-insight into the toxin-neuron interaction. *PLoS Pathog.* 2008; 4:e1000129. [PubMed: 18704164]
29. Schmitt J, et al. Structural analysis of botulinum neurotoxin type G receptor binding. *Biochemistry.* 2010; 49:5200–5205. [PubMed: 20507178]
30. Stenmark P, Dong M, Dupuy J, Chapman ER, Stevens RC. Crystal Structure of the Botulinum Neurotoxin Type G Binding Domain: Insight into Cell Surface Binding. *J Mol Biol.* 2010; 397:1287–1297. [PubMed: 20219474]
31. Strotmeier J, et al. Botulinum neurotoxin serotype D attacks neurons via two carbohydrate-binding sites in a ganglioside-dependent manner. *Biochem J.* 2010; 431:207–216. [PubMed: 20704566]
32. Zhang Y, Buchko GW, Qin L, Robinson H, Varnum SM. Structural analysis of the receptor binding domain of botulinum neurotoxin serotype D. *Biochem Biophys Res Commun.* 2010; 401:498–503. [PubMed: 20858456]
33. Strotmeier J, et al. The biological activity of botulinum neurotoxin type C is dependent upon novel types of ganglioside binding sites. *Mol Microbiol.* 2011; 81:143–156. [PubMed: 21542861]
34. Benson MA, Fu Z, Kim J-JP, Baldwin MR. Unique ganglioside recognition strategies for clostridial neurotoxins. *J Biol Chem.* 2011; 286:34014–34022.
35. Nuemket N, et al. Structural and mutational analyses of the receptor binding domain of botulinum D/C mosaic neurotoxin: Insight into the ganglioside binding mechanism. *Biochem Biophys Res Commun.* 2011; 411:433–439. [PubMed: 21749855]
36. Kozaki S, Kamata Y, Watarai S, Nishiki T, Mochida S. Ganglioside GT1b as a complementary receptor component for *Clostridium botulinum* neurotoxins. *Microb Pathog.* 1998; 25:91–99. [PubMed: 9712688]
37. Montecucco C. How do tetanus and botulinum toxins bind to neuronal membranes? *Trends Biochem Sci.* 1986; 11:314–317.
38. Nishiki T, et al. The high-affinity binding of *Clostridium botulinum* type B neurotoxin to synaptotagmin II associated with gangliosides GT1b/GD1a. *FEBS Lett.* 1996; 378:253–257. [PubMed: 8557112]
39. Kabsch W. XDS. *Acta Crystallogr D Biol Crystallogr.* 2010; 66:125–132. [PubMed: 20124692]
40. Collaborative Computational Project 4. The CCP4 suite: programs for protein crystallography. *Acta Crystallogr D Biol Crystallogr.* 1994; 50:760–763. [PubMed: 15299374]
41. Murshudov GN, Vagin AA, Dodson E. Refinement of macromolecular structures by the maximum-likelihood method. *Acta Crystallogr D Biol Crystallogr.* 1997; 53:240–255. [PubMed: 15299926]
42. Adams PD, et al. PHENIX: building new software for automated crystallographic structure determination. *Acta Crystallogr D Biol Crystallogr.* 2002; 58:1948–1954. [PubMed: 12393927]
43. Emsley P, Cowtan K. Coot: model-building tools for molecular graphics. *Acta Crystallogr D Biol Crystallogr.* 2004; 60:2126–2132. [PubMed: 15572765]
44. Strotmeier J, Willjes G, Binz T, Rummel A. Human synaptotagmin-II is not a high affinity receptor for botulinum neurotoxin B and G: increased therapeutic dosage and immunogenicity. *FEBS Lett.* 2012; 586:310–313. [PubMed: 22265973]

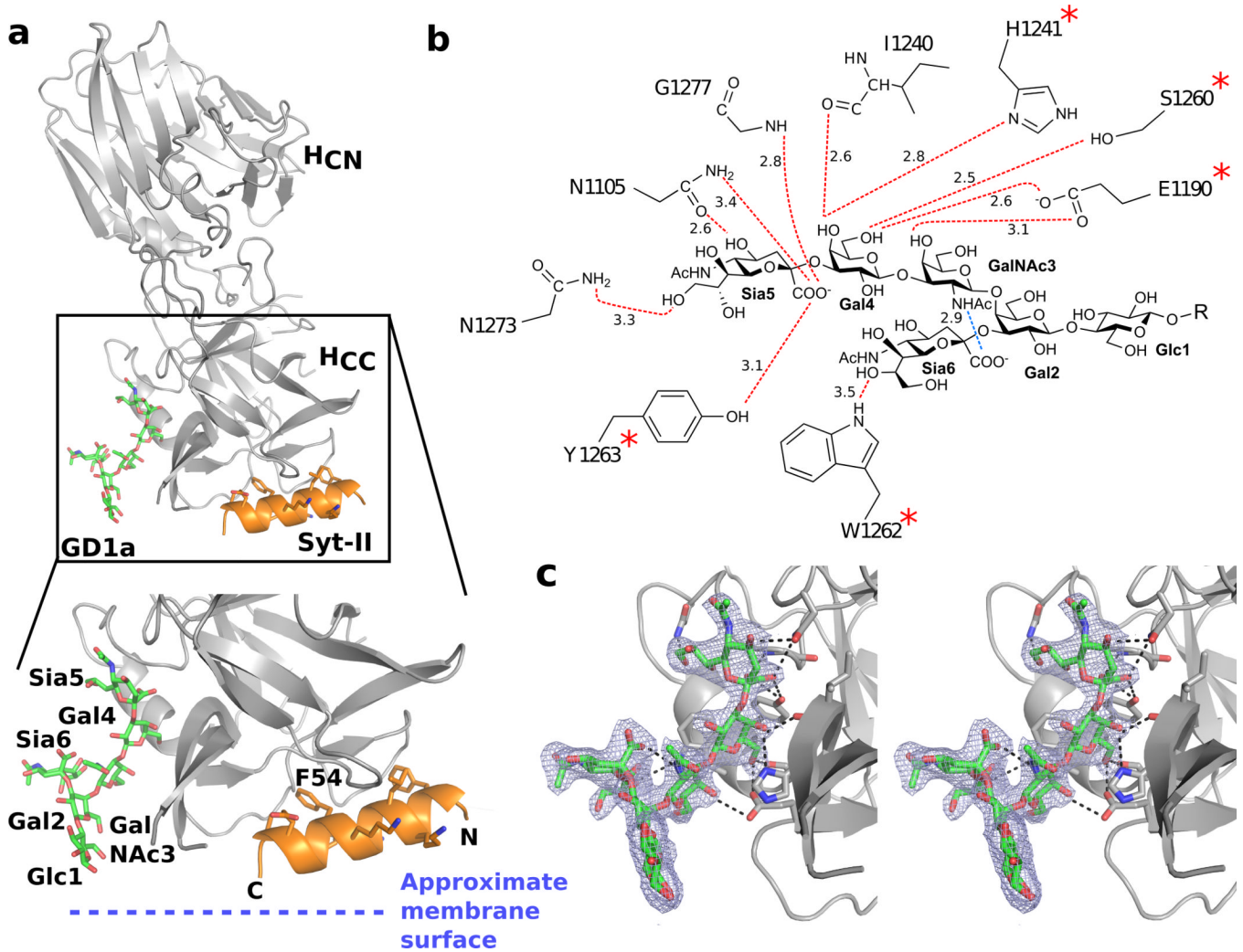


Figure 1. Dual receptor binding to BoNT/B
 (a) Overall view of BoNT/B (gray) with GD1a (green) and mouse Syt-II (orange) bound. Lower panel shows a close up view on the GD1a and Syt-II binding sites, with the GD1a moieties and the Syt-II residues, interacting with BoNT/B, shown as sticks. Phenylalanine 54 is indicated, this position is a leucine in human Syt-II that has a drastically lower affinity to BoNT/B than mouse Syt-II^{17,44}. (b) Schematic overview of possible hydrogen bonds between GD1a and BoNT/B (red dashed lines) and an internal hydrogen bond (blue dashed line). The hydrogen bond distance is shown for each bond (Å). Red stars show residues that previously, via mutagenesis, have been shown to be important for ganglioside binding²⁶. In GD1a, a ceramide is present at the R position, the GD1a oligosaccharide used here has a hydrogen in this position. (c) Stereo view of the bound GD1a, with its electron density ($2F_o - F_c$ map contoured at 1.5σ) in blue, and the possible hydrogen bonds to BoNT/B residues as dashed lines.

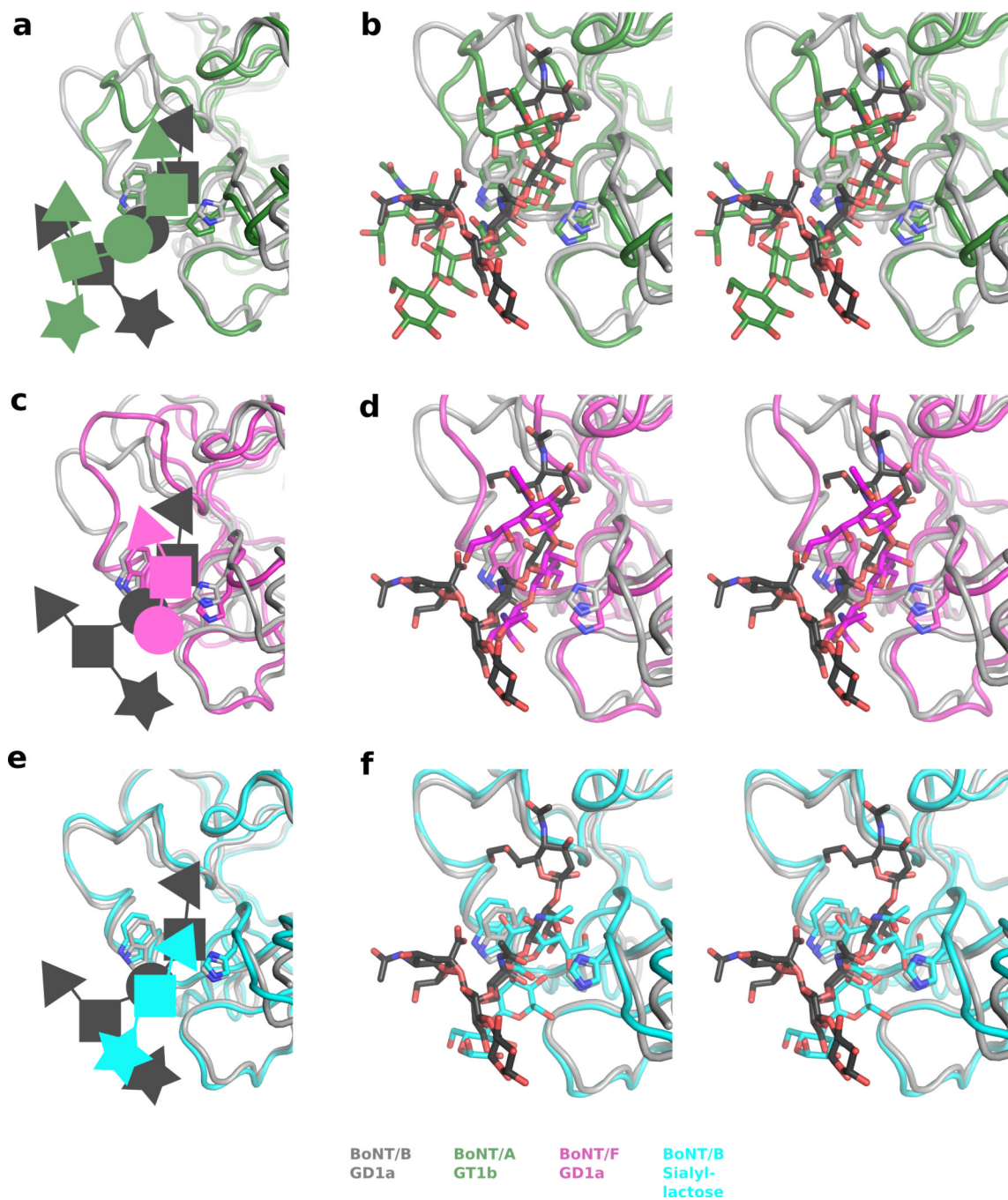


Figure 2. Comparison of the ganglioside binding to BoNT/B, BoNT/A and BoNT/F

The residues corresponding to W1262 and H1241 are shown in all structures. In the schematic panels (a, c & e) the individual sugar moieties are depicted as follows; triangles = Sia, rectangles = Gal, circle = GalNAc, star = Glc. In all panels BoNT/B with GD1a bound is depicted in gray and dark gray, respectively. The right hand panels (b, d & f) are stereo figures of the GBS. (a–b) Comparison to BoNT/A with GT1b (green, PDB code: 2VU9). (c–d) Comparison to BoNT/F and its bound GD1a (magenta, PDB code: 3RSJ). (e–f) Comparison to BoNT/B and its bound sialyllactose (cyan, PDB code: 1F31).

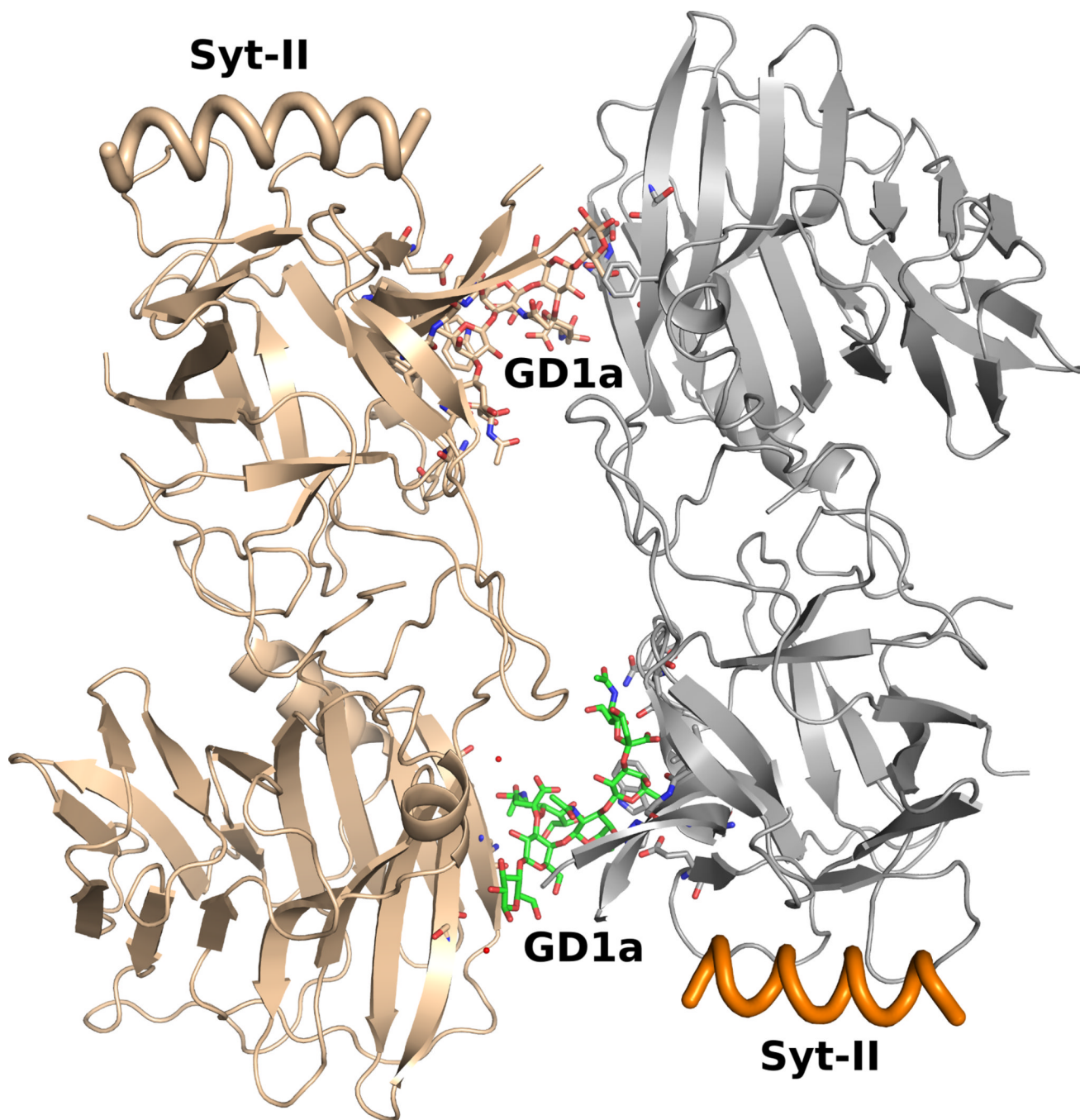


Figure 3. The asymmetric unit

The asymmetric unit containing two molecules of BoNT/B (gray), with the bound recognition domain of Syt-II (orange) and GD1a (green). The second copy of each molecule is colored in beige. All residues that interact with GD1a are shown as sticks. Crystal contacts are formed between the two BoNT/B protomers (gray and beige) in the asymmetric unit via the bound GD1a molecules. GD1a is bound to the GBS, as described in Fig. 1. The crystal contacts are formed by Glc1, Gal2 and Sia6. The green GD1a forms 3 hydrogen bonds, to S984, N1025 and L1022. The beige GD1a forms 5 hydrogen bonds, to S984, F986, N1025 and T1026. These interactions are not biologically relevant since BoNT/B has been shown to have a single GBS²⁶.

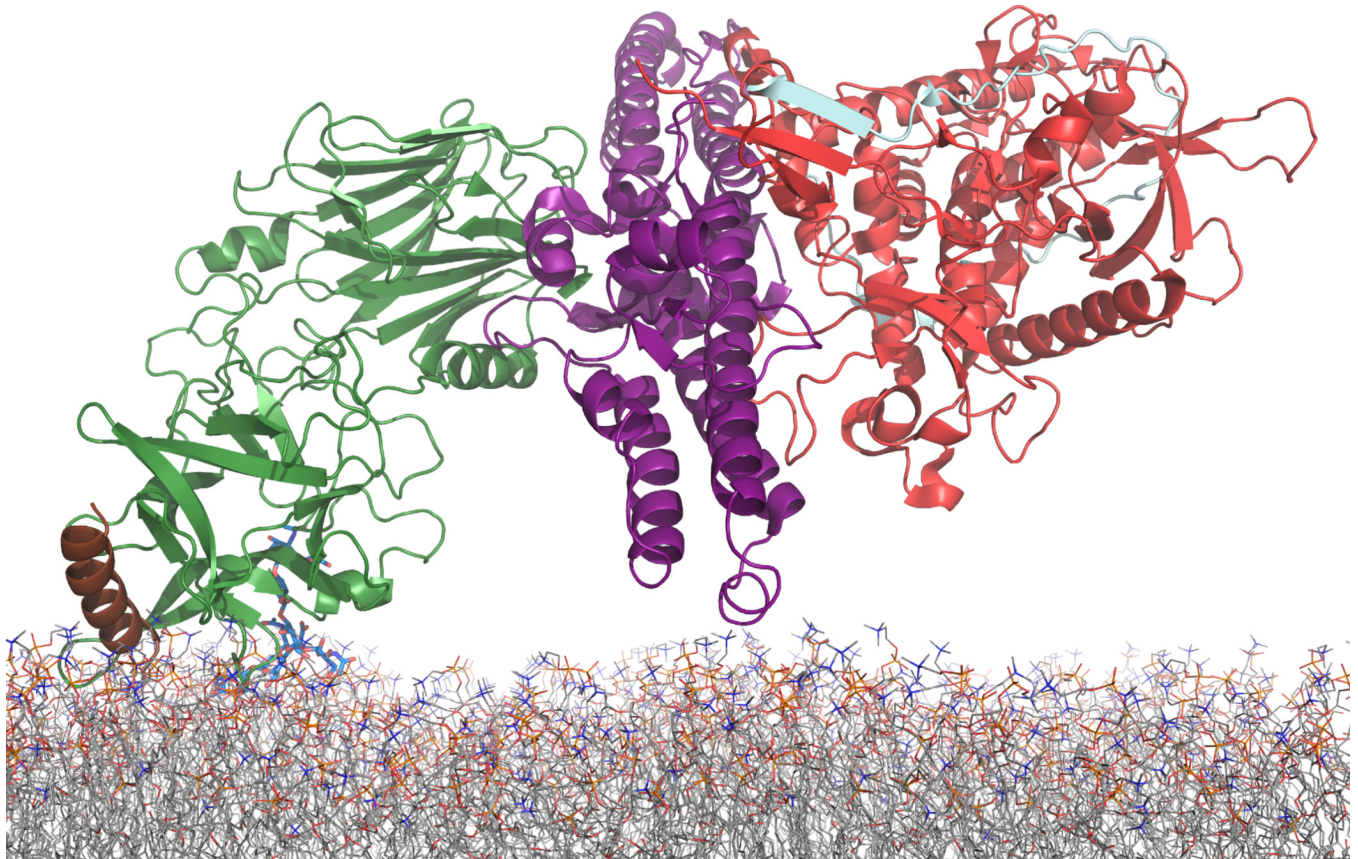


Figure 4. Model of BoNT binding to the neuronal membrane

The H_C (green), with its bound Syt-II (brown) and GD1a (blue), is from this study, while the H_N (purple) and LC (red) is superimposed using the structure of the entire BoNT/B (PDB code: 2NP0). The protein orientation is restricted by the binding of the two receptors. The structure presented here supports the entry of the translocation domain into the membrane with the end of the long helixes first^{22,28}. The regions linking both the protein receptor and ganglioside receptor to the membrane does allow for a certain degree of flexibility of the toxins orientation.

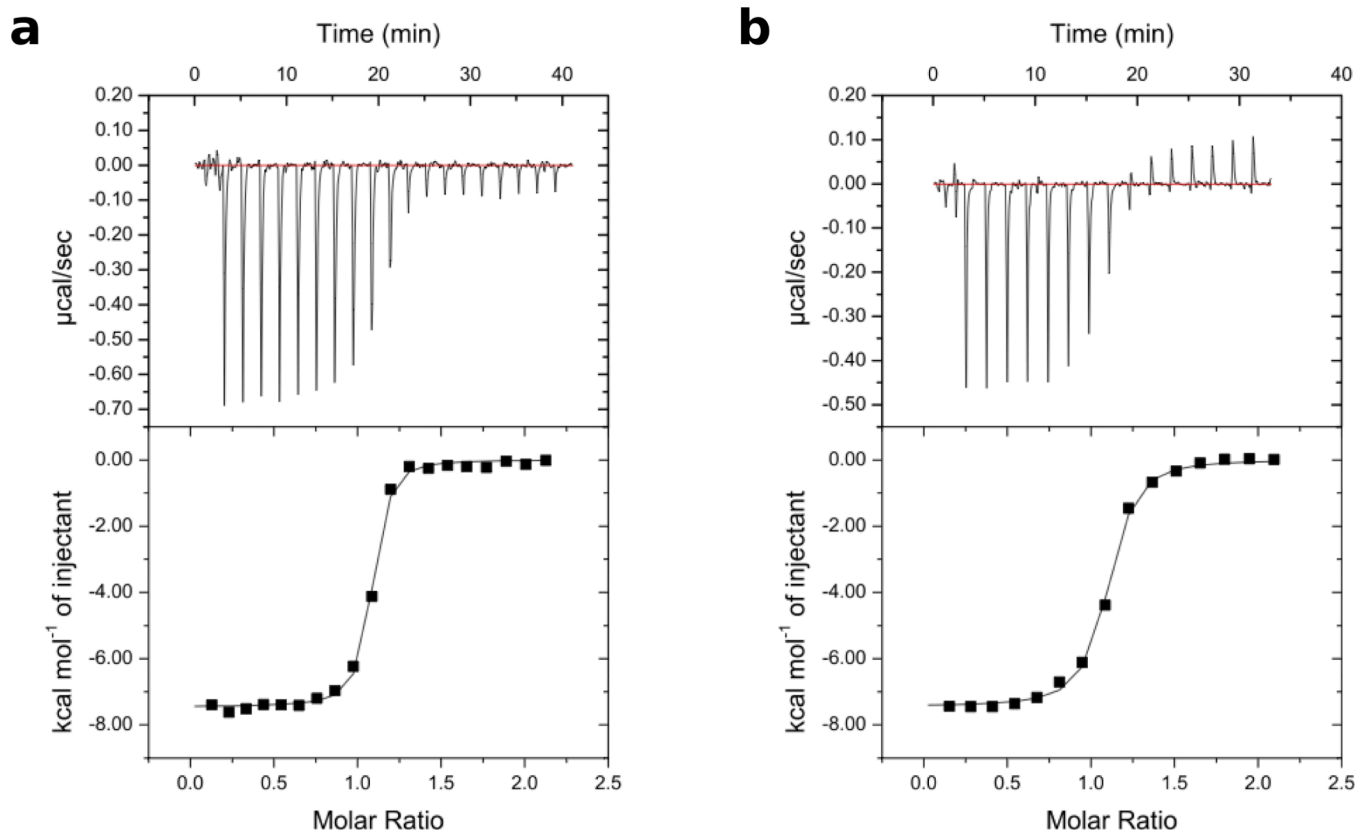


Figure 5. ITC titrations of Syt-II to BoNT/B

Representative ITC titrations of Syt-II to BoNT/B, without (a) and with (b) pre-incubation of $75 \mu\text{M}$ GD1a. (a) $K_D = 0.14 \pm 0.05 \mu\text{M}$ (b) $K_D = 0.18 \pm 0.06 \mu\text{M}$. The error is the standard deviation on at least two independent measurements. The baseline above zero in (b) is due to a slight buffer mismatch, and does not influence the calculated values.

Table 1

Data collection and refinement statistics

Data collection	
Space group	P2 ₁
Cell dimensions	
a, b, c (Å)	47.2, 158.2, 75.2
α , β , γ (°)	90.0, 108.4, 90.0
Resolution (Å)	44.7 – 2.3 (2.42-2.3)
R _{meas} (%)	14.1 (79.3)
I/ σ (I)	10.9 (2.3)
Completeness (%)	99.7 (98.5)
Redundancy	4.3
Refinement	
Resolution	44.7 – 2.3
No. unique reflections	50612
R _{work} /R _{free}	15.5 / 18.9
No. atoms	
Protein	7161
Syt-II ligand	284
GD1a ligand	176
Water	264
B-factors	
Protein	25.0
Syt-II Ligand	31.2
GD1a ligand	26.9
Water	21.1
R.m.s. deviations	
Bond lengths (Å)	0.008
Bond angles (°)	1.28

The data was collected from one crystal. Values in parenthesis are for the highest-resolution shell